

PCCP

Physical Chemistry Chemical Physics

Accepted Manuscript

This article can be cited before page numbers have been issued, to do this please use: P. Pramanik, R. Sahoo, S. Das and M. Halder, *Phys. Chem. Chem. Phys.*, 2020, DOI: 10.1039/D0CP03157G.



This is an Accepted Manuscript, which has been through the Royal Society of Chemistry peer review process and has been accepted for publication.

Accepted Manuscripts are published online shortly after acceptance, before technical editing, formatting and proof reading. Using this free service, authors can make their results available to the community, in citable form, before we publish the edited article. We will replace this Accepted Manuscript with the edited and formatted Advance Article as soon as it is available.

You can find more information about Accepted Manuscripts in the [Information for Authors](#).

Please note that technical editing may introduce minor changes to the text and/or graphics, which may alter content. The journal's standard [Terms & Conditions](#) and the [Ethical guidelines](#) still apply. In no event shall the Royal Society of Chemistry be held responsible for any errors or omissions in this Accepted Manuscript or any consequences arising from the use of any information it contains.

Fabrication of GUMBOS-based acid-base indicator: Smart probe for sensing acids and bases in any solvents

Prabal Pramanik^a, Rajkumar Sahoo^a, Sudhir Kumar Das^b, and Mintu Halder^{a}*

^aDepartment of Chemistry, Indian Institute of Technology Kharagpur, Kharagpur-721302, India.

^bDepartment of Chemistry, University of North Bengal, Darjeeling-734013, India.

Email: mintu@chem.iitkgp.ac.in

Abstract

This report embodies the synthesis of an ionic liquid-based pH-responsive indicator to sense acids or bases in non-polar as well as polar solvents. Herein, we have assembled a new ionic liquid (IL) comprised of a group of uniform materials based on organic salts (GUMBOS) by attaching quaternary phosphonium ionic liquid with very common acid-base indicator, methyl orange, via simple ion-exchange reaction. This integrated IL-based indicator is highly soluble in less polar solvents and exhibits good sensitivity towards the presence of acids/bases in those media. Further, this indicator has been exploited in determining the dissociation constants of several acids in non-aqueous aprotic solvents by overlapping indicator methods and hence provides essential information towards the understanding of many fundamental chemical reactions. This report has further scope for the synthesis of novel aqueous suspended nanomaterials, *i.e.* the nanoparticles derived from GUMBOS (nanoGUMBOS) by simple flash nano-precipitation method. The nanomaterial has been well characterized by different spectroscopic and microscopic studies. The obtained nanoparticles exhibit substantial pH-responsive behaviors in aqueous medium also and show better susceptibility as compared to the free organic indicator. Thus, this report explores the detailed studies on the IL-based indicator in sensing the acidity/basicity of various media.

Introduction

In recent days, great attention has been casted on designing and functionalization of new kinds of ILs-based sensors.¹⁻³ Unlike inorganic salts, *e.g.* NaCl, ionic liquids possess low melting points as their crystal lattice packing is disturbed due to the presence of two sterically mismatched ions.^{2,3} ILs have some unique properties like low melting point, low vapor pressure, less toxicity, biocompatibility, superior surface activity, antibacterial activity *etc.*, and hence they are used widely as the green solvents, reagents and also as catalysis in basic as well as applied research field.^{1, 3-7} ILs are better solvents than other commonly available solvents as they can solubilize most of the compounds and have low vapor pressure which allows to perform reactions in elevated temperatures.^{1, 8-10} The properties of an IL can be easily tuned as per applications by simple switching of their constituents or by addition of some specific functional groups.^{1-3,9} There are mainly two types of ILs: room temperature ILs (RTILs) which are liquid at room temperature (25 °C) and frozen ILs (FILs) which are solid at room temperature but melt below 100 °C. Warner and his coworkers have synthesized a new type of IL-based organic salts and defined them as group of uniform materials based on organic salts (GUMBOS).^{11, 12} They have suggested the melting point range of 25 °C to 250 °C for such GUMBOS. Hence the ionic salts having a melting point in between 25 °C to 100 °C are ILs as well as GUMBOS. Due to the significant properties, these GUMBOS systems become potential materials in various fields like extraction, separation, synthesis of sensors, biocatalysis, electrochemistry, fabrication of active pharmaceutical ingredients loaded drug carrier, microemulsion, energy conversion field and so on in recent days.³⁻⁵

In modern time, nanoparticles become a part of every corner of life due to some unique intrinsic properties like increased surface to volume reactivity compared to bulk samples, atomic

and electronic structure and some significant morphologies.^{4, 7, 13, 14} Recently, nanomaterials become the cutting edge of the biomedical research. They are utilized as therapeutics, cellular imaging, drug delivery systems and biological sensors.^{11, 15, 16} The use of ILs in synthesis of such biologically active nanomaterials as a template or solvent has gained high popularity in recent days.^{4, 17} The ionic liquids are highly capable to form cage-like hydrogen bonding which facilitates both self-organization and molecular-aggregation.¹⁸ The nanoparticles synthesized from GUMBOS (nanoGUMBOS) have various potential applications in biomedical world, sensing, energy conversion field *etc.*^{4, 11, 15, 19, 20} This report embodies the synthesis of an acid-base sensitive nanoGUMBOS which shows some remarkable properties compared to the bulk phase.

Any device that can mimic human gustatory and olfactory process is considered as an area of interest in past several decades.^{21, 22} Some expensive methodologies like NMR analysis, chromatography, mass spectroscopy, *etc.*, are available to investigate the properties of a medium. Among them, ratiometric spectroscopy-based as well as colorimetric sensors fabricated by different dye molecules which show distinct change in their color due to intermolecular interaction have gained immense interest in selective and sensitive analysis of a system rather than other types of sensors.^{8, 23, 24} Recently, ILs have been extensively used as potential materials in sensing of various biomolecules, gases, important ions, polarity of a medium *etc.*²⁵⁻²⁸ The Warner group has developed some IL-based optoelectronic sensors using pH indicator dyes which are effective in aqueous and vapor phases.⁸ Wang group has synthesized polymeric IL-based indicator to sense the presence of acids/bases in non-polar medium.²⁶ But to the best of our knowledge, there are no literature reports available till now which deals with the detailed spectroscopic investigation of the acidity along with the determination of acid dissociation

constant in any solvent. By keeping this fact in mind, present manuscript explores the detailed spectroscopic methods to estimate the dissociation constant of some acids using an IL-based indicator in non-polar medium for the first time.

The acid dissociation constant is one of the most significant and useful parameters in research world.²⁹⁻³⁷ There are plenty of reports on the determination of acid dissociation constant in protic solvents, but few are in less polar aprotic solvents.^{29-31, 36-38} In organic reaction, the knowledge of dissociation constants of an acid in non-aqueous aprotic non-polar medium is very much important. The solvents with high dielectric constant can reduce the electrostatic interaction between the proton and the conjugate base of an acid and allow them to be dissociated in the solvents.^{29, 39} But, in less polar solvent, this dissociation of an acid is not favorable. Hence determination of the degree of dissociation of an acid in less polar solvents is an area of immense interests of the scientists till date. There are some reports on the determination of the acid dissociation constant in non-aqueous systems. In most of the cases, measurements have been carried out conductometrically or potentiometrically where glass electrodes have been used, which includes lot of assumptions during the measurements.^{29, 38, 39} To avoid those associated problems, the best way is to apply overlapping indicator method to determine the prototropic dissociation constant of an acid/base in the aprotic less-polar solvents using some indicators.^{29, 40, 41}

In this report, we have synthesized a phosphonium IL-based methyl orange indicator by simple ion-exchange reaction. The synthesized IL-based indicator is highly soluble in less polar solvents (*e.g.* dichloromethane (DCM), acetonitrile (ACN) *etc.*), and shows high sensitivity towards the presence of acids or bases in those solvents. Further, this ionic liquid has also been exploited to determine the dissociation constant of several acids in less polar aprotic solvent.

Herein, we have adopted overlapping indicator methods to determine the absolute acidities of some acids in acetonitrile.³⁰ Moreover, we have synthesized aqueous suspended nanoparticles (nanoGUMBOS) from this prepared IL by flash nano-precipitation method in order to utilize the indicator in aqueous medium also. This indicator nanoparticles further show better color change in naked eye compared to the free organic indicator molecules. Thus the report represents a complete account on the designing of an acid-base sensitive indicator acting in polar as well as non-polar media and exploration of such systems in determining the absolute dissociation constant of several compounds in those media.

Experimental sections

Materials

Methyl orange (MO) and trihexyltetradecylphosphonium chloride ($P_{66614}Cl$) (>95%) have been purchased from Sigma Aldrich. All the acids and solvents used are of analytical reagent (AR) grade obtained from Merck, India. All the solvents have been dried further before use. All the glasswares were thoroughly washed by concentrated sulfochromic acid followed by repeated washing with water.

Preparation of ionic liquid-based indicator and nanoparticles

The methyl orange based ionic liquid (MOIL) indicator was synthesized by previously reported mechanism with some modifications.^{8, 42} Briefly, methyl orange dye and $P_{66614}Cl$ ionic liquid were taken in equimolar ratio in a mixture of DCM - Water of 2:1 (v/v) ratio. The mixture was stirred overnight. The color of the DCM layer (bottom layer) was changed from colorless to red and the water layer (upper layer) became colorless indicating the successful ion-exchanged process. The DCM layer was washed by water several times to remove the byproduct, NaCl

completely. The complete removal of NaCl was confirmed by the addition of AgNO₃ to a part of the aqueous layer until no white precipitate due to formation of AgCl appeared. The above aqueous layer was discarded out. Anhydrous Na₂SO₄ was added further to the system to absorb water present in the DCM layer. DCM layer was then filtered. MOIL indicator was obtained by evaporating DCM and remaining water under vacuum at ~80 °C. We have further lyophilized the material thoroughly to remove water molecules completely. The synthesized indicator (MOIL) was characterized by NMR, HRMS, FTIR, and UV-vis spectra.

We have adapted simple flash nano-precipitation methods for the preparation of MOIL nanoparticles (MOIL NP). A stock solution of 1 mM of MOIL in DMSO (good solvent) was prepared by dissolving requisite amount of the indicator in DMSO. Different aliquots of the stock solution were then injected rapidly in triply distilled water followed by sonication for nearly 15 minutes resulting the formation of nanoparticles in the aqueous medium. The prepared nanoparticles have been characterized by FESEM, AFM, DLS, and spectroscopic studies.

Instrumentations

Field emission scanning electron microscopy (FESEM) images were recorded using a FEI NOVA NANOSEM 450 with an operating voltage of 5 kV. A freshly prepared aqueous MOIL NP sample was drop casted on the glass side and coated with gold particles by a sputter coater. Atomic force microscopy (AFM) measurement was performed in Agilent Technologies, Model 5500. Fourier transform infrared spectroscopic (FTIR) measurements were conducted with a Perkin-Elmer FTIR spectrophotometer. Dynamic light scattering (DLS) analyses were carried out by Malvern Nano ZS (model no. ZEN3600) instrument where the data were recorded by a 4 mW He – Ne laser ($\lambda = 632$ nm). The UV-vis absorption spectra were recorded using a Shimadzu UV-2600 absorption spectrophotometer equipped with a TCC-260 thermoelectrically

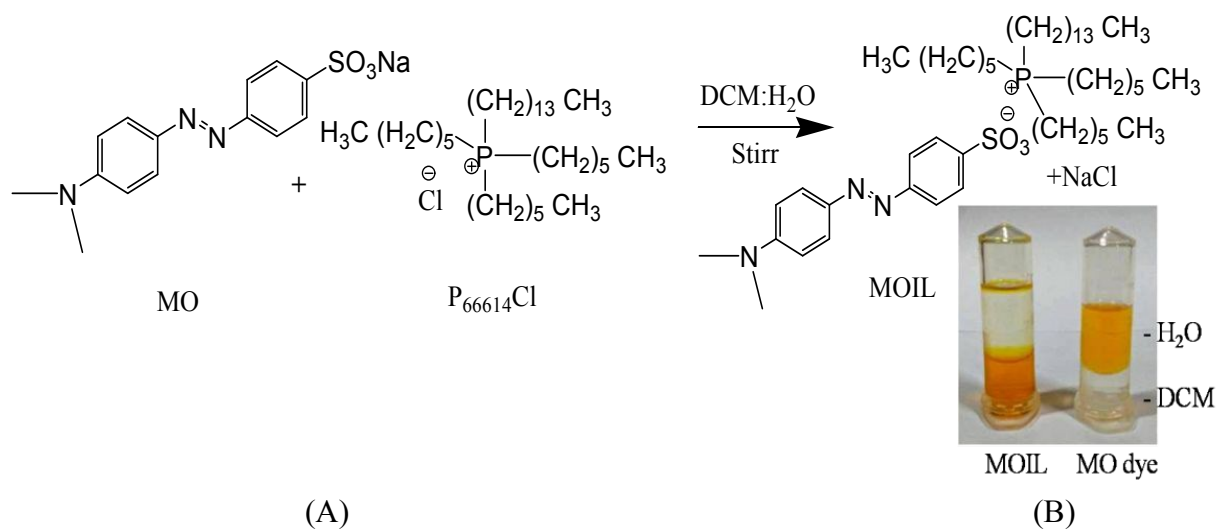
temperature-controlled cell holder in the wavelength range of 200-800 nm by scanning freshly prepared solution taken in a cuvette of 1 cm path length. During acidic titration experiments, acids were added gradually to a definite volume indicator solution and the absorbance of the solution was recorded after each addition. During titration, volume correction was performed after every addition of acid. Here, we have chosen those acids which do not have any absorbance in the examined region. Differential scanning calorimetry (DSC) measurement was conducted using Tzero aluminum pan in Thermal Analysis (DSC Q20) instrument with a scan rate of 2 °C min⁻¹ in the range of -50 °C to 230 °C under nitrogen atmosphere.

Results and Discussion

Characterization of synthesized ionic liquids

The synthesized MOIL has been characterized by several spectroscopic and calorimetric techniques. Nuclear magnetic resonance (NMR) studies have confirmed the successful synthesis of MOIL via ion-exchange reaction (Fig. S1-3, data are given in the Supporting Information). In the FTIR spectrum of MOIL (Fig. S4), the two bands located at 2953 & 2925 cm⁻¹ are the characteristic peaks for asymmetric stretching, and the two bands at 2871 & 2855 cm⁻¹ are the characteristic peaks for symmetric stretching of C-H function group of the long aliphatic chain present in cationic phosphonium moiety.⁴³ The bands at 1603 and 1519 cm⁻¹ are due to aromatic C=C stretching; the band at 1422 cm⁻¹ is attributed to N=N stretching, and the band appeared at 1364 cm⁻¹ is due to sulfonate group of methyl orange moiety.⁴⁴ FTIR spectrum thus suggests the formation of MOIL by the incorporation of phosphonium IL and methyl orange entities. High resolution mass spectroscopy (HRMS) study of MOIL was performed in positive and negative

ion mode (Fig. S5A-B). Two significant peaks at 483.5053 (m/z) (positive ion mode) and 304.0762 (m/z) (negative ion mode) are assigned to the characteristic peaks of cationic phosphonium backbone and anionic methyl orange moiety, respectively. Hence HRMS spectra confirm the formation of the ionic salt (MOIL) by equimolar incorporation of two oppositely charged entities and the molecular weight of MOIL is estimated to be 788.2 Da from the HRMS analysis for equimolar incorporation. The exchange ratio of chloride ions by MO moieties is almost 100 %, *i.e.* most of the chloride ions of $P_{66614}Cl$ have been exchanged by the anionic moiety of methyl orange to form $[P_{66614}]^+[MO]^-$ (MOIL). Scheme 1A provides the synthetic route of MOIL.⁴⁵ At room temperature, MOIL is found to be sticky solid. To check whether the synthesized ionic salt follows the condition for being an IL *i.e.* the melting point should be < 100 °C, we have performed differential scanning calorimetry (DSC) study. DSC spectrum shows that the ionic salt has a sharp melting point at ~ 35 °C (Fig. S6). Hence the synthesized MOIL ionic salt is an IL as well as GUMBOS as it has a melting point in between 25 °C to 100 °C.¹²



Scheme 1. (A) Synthetic route of MOIL indicator. (B) Solubility of MO dye and MOIL in a mixture of DCM-water (1:1 v/v ratio).

According to Scheme 1A, the Na^+ ion of MO dye is replaced by the long-chain lipophilic cationic phosphonium backbone. This introduces hydrophobicity to the whole systems and as a result the synthesized indicator (MOIL) is highly soluble in less polar solvents (such as dichloromethane, chloroform, hexane *etc.*) while they are insoluble in polar solvent like water. The electrostatic attraction between the cationic phosphonium moiety and the sulfonate group of the MO moiety is strong enough that they cannot be ionized or solubilized in the polar solvents. Scheme 1B represents that the indicator MOIL is only soluble in dichloromethane (DCM) solvent and could not be solubilized in aqueous medium while the normal MO dye is soluble only in water medium. A mixture of 1:1 (v/v) of DCM : water containing MOIL indicators was ultrasonicated for 2 h followed by nightstand. No significant absorbance of MO moiety was found in the aqueous phase indicating that the attraction between the negative moiety of MO dye and the positive backbone of the IL is very strong and hence cannot be dissociated by simple sonication methods. To define the hydrophobicity of the synthesized MOIL, we have determined the 1-decanol/water ($K_{o/w}$) partition coefficient of MOIL following a standard procedure.¹¹ The $K_{o/w}$ of MOIL is estimated to be 17.5 ± 0.5 which suggests that the compound has strongly hydrophobic nature. Therefore, the solubility of MOIL in water is negligible. However, it has been stated elsewhere that the solubility of water in phosphonium ionic liquids can be quite high.⁴⁶⁻⁴⁸ Schlosser group has stated that up to 8 water molecules can be accommodated by one phosphonium ionic liquid molecule and the presence of water affects many physical properties (like density, viscosity *etc.*) of the ILs.^{46, 47, 49} The presence of water molecules in our indicator may affect the results. Hence, we have attempted to estimate the water content present in our prepared system by oven-drying methods.^{50, 51} A definite amount of MOIL has been dried in oven increasing the temperature from 50 °C to 150 °C for 10 h and maintaining the final

temperature for 3 h under low pressure. Under such condition, we may assume that all the water molecules get evaporated and the water content present within the sample should be now negligible.⁵¹ From the loss in mass due to evaporation of water, we may estimate the mass percentage of water present in the prepared MOIL. The mass percentage of water present in prepared MOIL is estimated to be less than 1.0 % at 25 °C indicating that the prepared IL is almost dry, and hence the indicator can be used in determining the acidity of a medium with minimal error. We have further investigated the solubility of water in the prepared IL. A ternary system has also been prepared by dissolving water in a mixture of MOIL and benzene of different w/w ratio. Here, the solubility of MOIL and benzene in water is considered as zero. It has been found that the three-phase system present in very narrow concentration region in ternary MOIL-benzene-water mixture (Fig. S7A). The relative molar fraction of the ionic liquid (X_{IL}) in the solvents in absence of water is estimated by the following eqn (1).

$$X_{IL} = \frac{x_{IL}}{x_{IL} + x_{Benzene}} \quad (1)$$

Here, x_{IL} and $x_{Benzene}$ are referred to their corresponding molar fraction in the ternary system. From the plot of x_{water}/x_{IL} vs X_{IL} (Fig. S7B), we have found that the water/IL molar fraction ratio increases initially with increase in the concentration of MOIL in the solvent and then gets saturated. The result indicates that up to $X_{IL} = 0.1$, nearly 3 water molecules can be accommodated with one IL ion pair.^{46, 51}

The pH-responsive behavior of MOIL in less-polar solvents

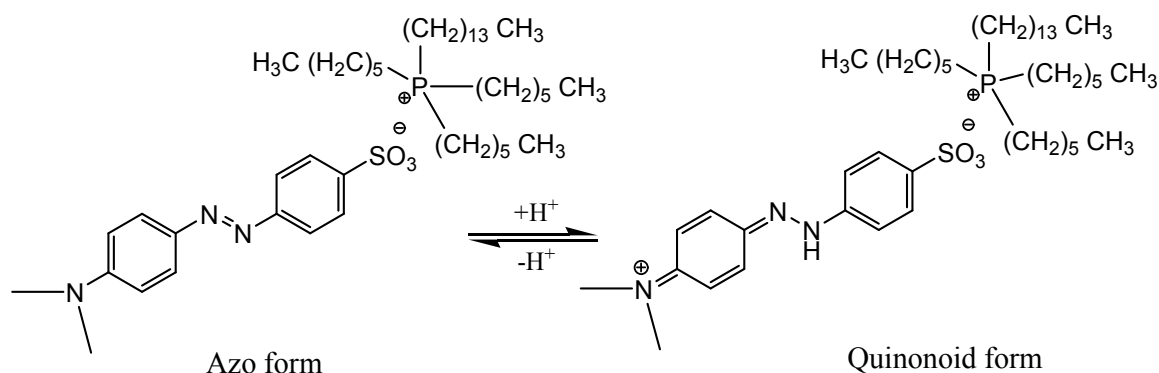
The absorption spectrum of MOIL was recorded in less polar solvents. The absorption spectrum is mainly generated by the indicator moiety as the phosphonium IL moiety does not have any absorbance in our examined region. It was found that the absorption spectrum of MOIL

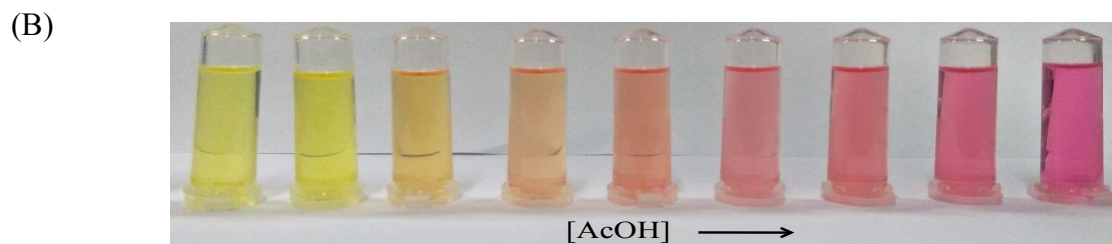
is nearly similar to that of free MO dye in dimethyl sulfoxide (DMSO) (Fig. S8A). This further confirms that the chemical structure of MO moiety in MOIL is not affected during ion-exchange reaction. The interaction between the dye moiety and the phosphonium backbone is highly electrostatic nature and the chemical structure of MO moiety remains unaltered within the system. In DCM, a little blue shift was observed in the absorption maximum of MOIL ($\lambda_{\max} \sim 415$ nm) with respect to that of free MO dye in DMSO ($\lambda_{\max} \sim 430$ nm). This blue shift in the absorption spectrum in case of MOIL can be attributed to the positive solvatochromism in less polar solvents.⁵²

The absorbance of MOIL was studied in DCM in presence of various acids (Fig. 1A-D). Due to pH-responsive behavior of MO dye, MOIL is also expected to show such behavior in less polar solvents. For comparison, we have recorded the absorption spectra of free MO dye in aqueous medium. The color of MO dye is dependent on the percentage ratio of the azo (benzinoid) form and quinonoid (zwitterion) form present in the system as the two forms absorb light in two different region.⁵³ In neutral water, MO dye remains only in azo form and exhibits a single absorption band having maximum at ~ 464 nm. With the addition of an acid to the system, the azo form is gradually converted to quinonoid form. As a result, the absorbance corresponding to the azo form (at ~ 464 nm) decreases gradually with a concomitant increase in the absorbance at ~ 508 nm which is the characteristic absorption peak of the quinonoid form (Fig. S8B). We may expect same kind of mechanism for MOIL also. We found that in neutral DCM, the absorption spectrum of MOIL contains single band (λ_{\max} is ~ 415 nm) suggesting that the indicator exists only in azo form in neutral condition. With the addition of acids which are soluble in less polar solvents [CH_3COOH (AcOH), and CF_3COOH (TFA) here] the azo form of the indicator is gradually converted to the quinonoid form (mechanism illustrated in Scheme

2A). As a result, a distinct color change from yellow to fuchsia was observed by naked eyes (Scheme 2B). This is well reflected in the absorption spectra (Fig. 1A-D), where the absorbance of the azo form ($\lambda_{\text{max}} \sim 415$ nm) gradually decreases while the absorbance of the quinonoid form at longer wavelengths ($\lambda_{\text{max}} \sim 523$ nm) increases with the addition of acids. A distinct isosbestic point ($\lambda \sim 470$ nm) was found in the absorption spectrum of MOIL (Fig. 1A&C) indicating the presence of equilibrium during the conversion from azo to quinonoid form. In case of MOIL, the spectral shift for the conversion of azo to quinonoid form in DCM (spectral shift: from 415 nm to 523 nm, ~ 108 nm) is more than twice to that of free MO dye in water (spectral shift: from 464 to 508 nm, ~ 44 nm). This result indicates that MOIL shows better color change in naked eyes (yellow to fuchsia) in less polar solvents than MO dye (orange to red) in aqueous medium. Thus, the prepared MOIL indicator exhibit better pH-responsive behavior compared to free dye. On careful observation, it was found that the addition of little amount of weak acid (CH_3COOH) to a solution of MOIL in DCM causes a small increase in the absorbance corresponding to the azo form along with a small red shift and this is not observed in case of MO dye. This perhaps due to the fact that the small amount of acid may increase the solvent polarity within the non-polar environment and hence MO moiety within MOIL displays better color in the solution.²⁶

(A)





Scheme 2. (A) Mechanism of acidic conversion of MOIL, and (B) color change of MOIL in presence of AcOH in DCM.

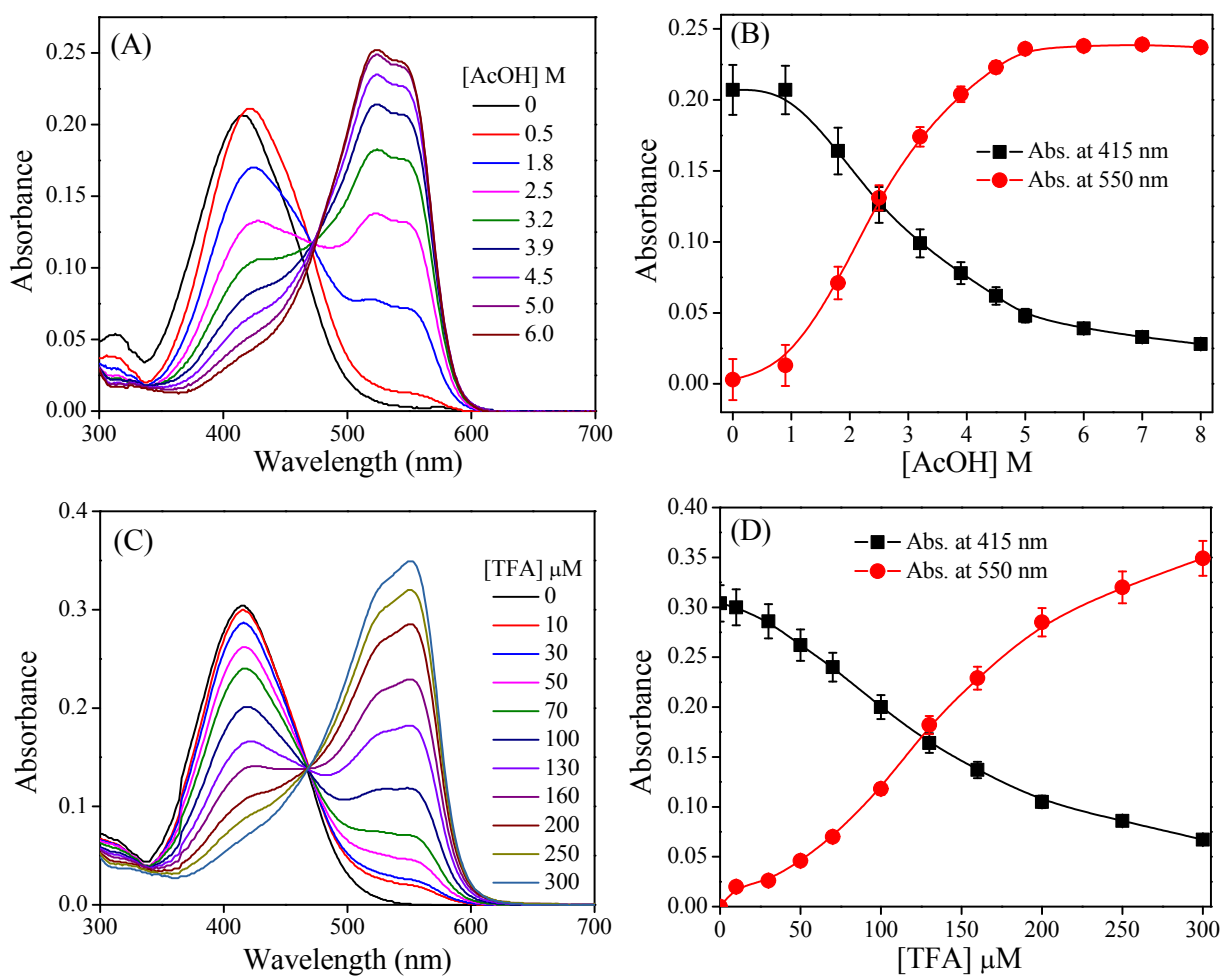


Fig. 1. (A) & (C) UV-vis absorption spectra of MOIL in presence of AcOH and TFA in DCM, and (B) & (D) change in absorbance of MOIL as a function of different acid concentration, respectively.

In this report, acetic acid (Fig. 1A&B) and trifluoroacetic acid (Fig. 1C&D) were used as a source of acid. In both cases, the concentration of the acids required for the complete conversion of the azo form of MO moiety in MOIL to its quinonoid forms are much higher than that required in aqueous medium. This is mainly due to the low degree of dissociation of an acid in less polar solvents compared to water as the ionization of an acid is highly facilitated by the higher solvent polarity.^{26, 36, 39, 54} Fig. 1B&D show that the absorbance of the azo as well as quinonoid form of MOIL changes sigmoidally with the concentration of acids. We found that our prepared indicator, MOIL shows good acid sensitivity in non-polar solvents compared to other similar kinds of indicator.²⁶

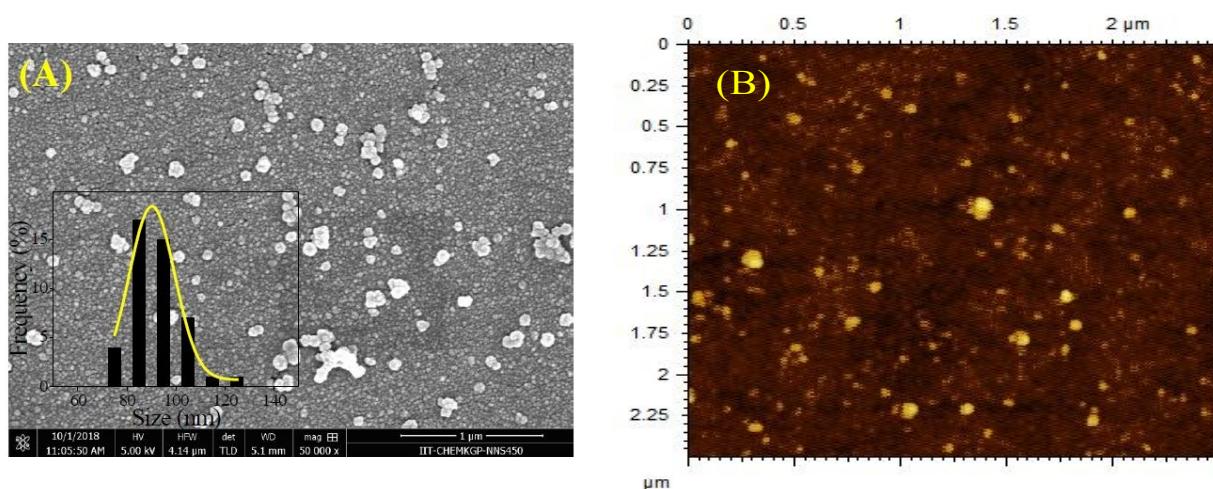
In this report, we have also investigated the effect of concentration of the prepared indicator towards the sensitivity of acids present in the system. Considering 788.2 Da as the molecular weight of MOIL for equimolar incorporation, confirmed by the HRMS study, we have prepared several concentrated solutions of MOIL (5 to 100 μM) for acidic titration experiments. It was observed that the amount of weak acids (AcOH here) required for the complete conversion of indicator molecules from its azo to quinonoid form is proportional to the concentration of the indicator present in the systems, *i.e.* higher amount of acid should be required for the complete conversion in case of higher concentrated solution of MOIL compared to low concentrated solutions (Fig. S9). Here, we have chosen a 20 μM MOIL solution for all the following acidic titration experiments as it exhibits prominent color change in naked eyes with profound acid sensitivity in DCM medium. MOIL exhibits similar kind of behaviors in other less polar solvents like chloroform, benzene, acetonitrile *etc.* (Fig. S10) making it a fundamental probe for determining the acidities of various solvents.

Characterization of MOIL nanoparticles

To investigate the pH in polar medium like water, we have synthesized aqueous suspended MOIL indicator nanoparticle (MOIL NP), *i.e.* a nanoGUMBOS, from the prepared IL-based GUMBOS by simple flash nano-precipitation method. We want to explore the acid sensitivity of such nanoGUMBOS systems in aqueous medium in comparison with the free dye molecule. MOIL contains a long hydrophobic side chained IL backbone. Therefore, it has high tendency to form nanoaggregates when a little amount of MOIL solution, prepared in DMSO (good solvent), is injected in aqueous medium (poor solvents). It has been reported elsewhere that the covalent and non-covalent interaction, here π - π interaction, are responsible for the molecular aggregation in nanoscale level.⁵⁵ The properties and morphologies of the nanoparticles are highly dependent on several parameters like concentration, temperature, pH of the medium *etc.* Here, we have investigated the effect of concentration upon the size and properties of the nanoparticles. For this, different amounts of DMSO stock solution of MOIL (1 mM) were injected into water at room temperature followed by ultrasonication (\sim 15 minutes) to prepare different concentrated (net) solutions (5 to 100 μ M) of the nanoparticles. We have found that the MOIL NPs in 10 μ M solution possess minimum average hydrodynamic size in aqueous medium with a high positive surface charge (zeta potential is 5.2 ± 0.5 mV) (Fig. S11). High zeta potential value indicates that the nanoparticles are quite stable in aqueous medium. Below this concentration, the size of the nanoparticles increases due to lower zeta potential value; while above this concentration, the size again increases as large nanoaggregates are formed in such conditions [Fig. S11A, inset]. Later, we have found that the indicator nanoparticles of this concentration (10 μ M) exhibit very good sensitivity towards the presence of acid in naked eye, and hence, we have chosen the 10 μ M MOIL NP solution for following experimental analyses.

We have also found that the MOIL NPs of other concentrations show similar kind of sensitivity, and the concentration does not impact much on their acid sensitivity.

The synthesized MOIL NP (10 μM) was characterized by several spectroscopic and microscopic methods like FESEM, AFM, DLS, UV-vis studies *etc.* FESEM study (Fig. 2A) confirms the formation of the nanoparticles which have nearly spherical shape with an average size of 90 ± 10 nm and they are well dispersed in aqueous medium. AFM spectrum also confirms that the molecular aggregations are in nanoscale level (<100 nm) (Fig. 2B). We have further determined the size of the prepared nanomaterials in aqueous medium by DLS methods and found that the average hydrodynamic size of the MOIL NP lies in nanometer range (130 ± 10 nm) (Fig. 2C).



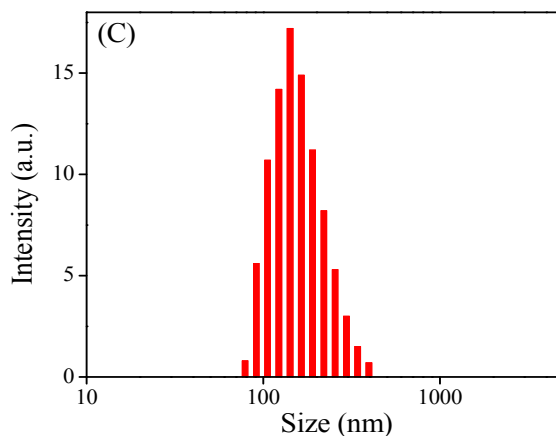


Fig. 2. (A) FESEM image, (B) AFM image, and (C) DLS spectrum of MOIL nanoparticles.

Absorption spectrum of MOIL nanoparticles in water has been recorded and compared with the parent compound. A slight blue shift was observed in the absorption spectrum of MOIL NP in aqueous medium ($\lambda_{\text{max}} \sim 421$ nm) compared to MOIL in DMSO medium ($\lambda_{\text{max}} \sim 428$ nm) (Fig. 3A). Due to charge transfer transition in electron donor-acceptor (EDA) systems like methyl orange, a bathochromic shift in the absorption spectrum is expected to be observed with the increase in the polarity of a medium.⁵⁶ But we found a hypsochromic shift in the absorption spectrum of MOIL NP in aqueous medium which can only be attributed to the H-type aggregation of the MO moieties within the nanoaggregate.⁵⁶⁻⁵⁸ Further, in order to confirm the fact that the phenomenon is an aggregation effect, not just an inherent property of the nanoGUMBOS system, concentration-dependent absorption spectra of the freshly prepared nanoparticles were recorded. A gradual blue shift was observed in the absorption spectrum with the increase in the nanoparticle concentration (Fig. 3B). This result further confirms the aggregation process where the methyl orange moieties are oriented as to have head-to-head interaction, *i.e.* the H-type aggregation within the nanoaggregates.

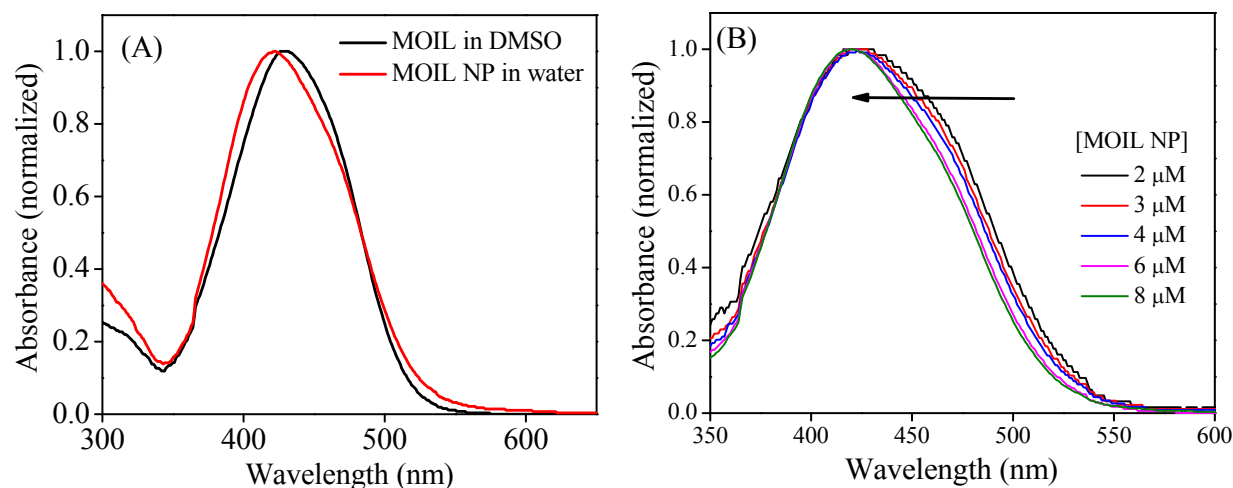


Fig. 3. (A) Absorption spectra of MOIL and MOIL nanoparticle (10 μM) in DMSO and water, respectively. (B) Absorption spectrum of MOIL NP with concentration variation in water.

pH-responsive behavior of MOIL nanoparticles in polar medium

The pH-responsive behavior of the prepared MOIL NP has been further investigated in aqueous medium. The MOIL NP exhibits remarkable pH-responsive behavior compared to free MO dye in water. The nanoparticles exhibit maximum absorbance at ~ 421 nm (Fig. 4A) in neutral aqueous medium which is attributed to the absorbance corresponding to the azo form of the MO moiety. The absorption spectrum is significantly blue shifted compared to that of methyl orange dye in water ($\lambda_{\text{max}} \sim 464$ nm). The large blue shift (~ 43 nm) indicates that the MO moieties may remain in a hydrophobic environment within MOIL nanoGUMBOS system synthesized from long-chain lipophilic ionic liquids, and the dye moieties are aggregated in H-type fashion within the nanoaggregate. This is also supported by the zeta potential studies. From zeta potential measurements, we have found that the nanoparticles have positively charged surface. This suggests that the negatively charged methyl orange units may remain inside the hydrophobic cavity formed by the long-chain backbone of the positive phosphonium moiety.

Hence a large blue shift is observed in case of MOIL NP compared to free MO dye in aqueous medium. With the addition of acid (CH_3COOH here), the dye moieties of MOIL nanoGUMBOS are gradually converted from their azo to quinonoid forms and hence a distinct color change is observed from yellow to red. This is further observed in the absorption spectrum where the absorption attributed to the azo form of the dye ($\lambda_{\text{max}} \sim 421 \text{ nm}$) is gradually decreased with a concomitant increase in the absorbance at $\sim 511 \text{ nm}$ corresponding to the quinonoid form with the gradual addition of acids to the aqueous solution of MOIL NP. A distinct isosbestic point has been observed at $\sim 465 \text{ nm}$ suggesting the presence of equilibrium in between the azo and the quinonoid forms of the dye moieties. For comparison, the absorption spectra of free dye molecule have been collected in both acidic and basic medium (Fig. 4B). The spectral shift for azo to quinonoid conversion in case of MOIL NP covers 421 nm to 511 nm ($\sim 90 \text{ nm}$) which is twice as compared to free MO dye ($\sim 44 \text{ nm}$). Hence, our synthesized indicator nanomaterial provides wider range of color change in naked eye during acid-base titration compared to free methyl orange indicator; MO dye changes its color from orange to red while MOIL NP changes its color from yellow to red. Therefore, such type of nanomaterials can be served as better pH-responsive indicator compared to free organic dyes. We have also assessed the reversibility of our synthesized indicator nanoparticle and found that the conversion between azo to quinonoid form is a reversible process like free dye molecules. Hence, such type of nanoGUMBOS system can be useful materials in designing the optoelectronic pH sensors rather than using bulk organic dyes.

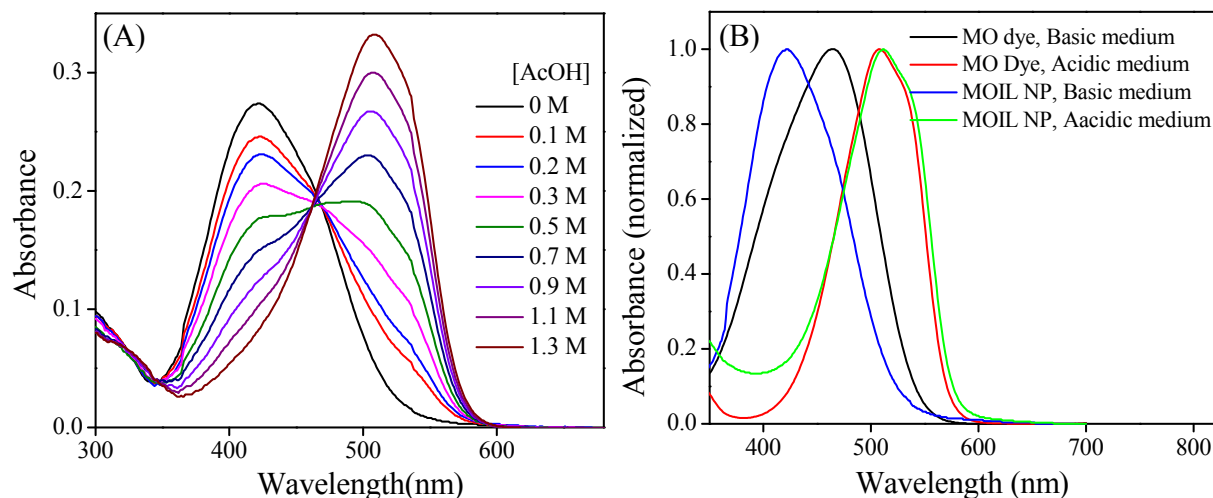


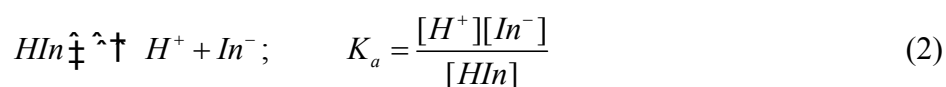
Fig. 4. (A) Absorption spectra of MOIL NP as a function of AcOH concentration, and (B) comparative spectral shift of MOIL nanoparticle and free MO dye in water.

Determination of pK_a of several acids in non-polar solvents

Equilibrium acidities of some acids have been measured using the prepared indicator, MOIL in this report spectrophotometrically in aprotic less-polar solvents, here acetonitrile. There are plenty of articles on the determination of the acid dissociation constant of several acids in non-aqueous solvents.^{29-31, 36-38} In most of the cases, measurements are performed by conductometric or potentiometric methods using glass electrodes as the pH electrodes.³⁵⁻³⁸ But the relation between the glass electrode potential with the acid strength is estimated theoretically in non-polar aprotic medium which has several assumptions, and hence the estimation procedure may not give us the accurate result.²⁹ Till date, the quantitative information about the acid-base equilibrium and the knowledge of acidity in the non-aqueous solvents are incomplete. The best way to determine the equilibrium constants of an acid in the aprotic less-polar solvents is to use of an indicator.^{29, 40, 41} Using an indicator of known equilibrium constant (pK_{HI_n}), it is easy to

determine the acidity of a medium spectrophotometrically. In UV-vis spectrophotometric measurements, low concentration of acids or base can be used which can avoid the other unwanted competing processes.

The molar extinction coefficient (ϵ) of HIn (quinonoid) form of MOIL indicators was determined by Lambert-Beer's law under excess acidic condition in acetonitrile. The ϵ of HIn form is estimated to be $(25.5 \pm 0.5) \times 10^3 \text{ M}^{-1}\text{cm}^{-1}$ (measured at 520 nm). We have determined the pK_{HIn} of MOIL in acetonitrile by direct spectroscopic methods using the following relations.



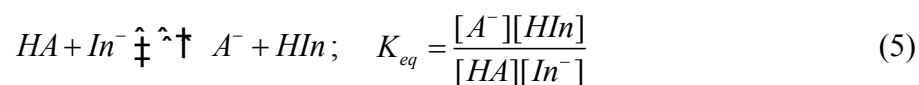
$$\text{pH} = \text{p}K_a + \log \frac{[\text{In}^-]}{[\text{HIn}]} \quad (3)$$

During calculation of the pK_{HIn} , we have considered the acid dissociation constant of the weak acids, CH_3COOH , as the reference ($\text{p}K_a = 23.51$) to determine the pH of the medium.^{34, 40} Different aliquots of AcOH was added to a solution of MOIL of known concentration in acetonitrile and the corresponding concentration of HIn present in the medium was estimated by the characteristic molar extinction coefficient value in each step. The concentration of the remaining species (In^-) can be determined using eqn (4). From the plot of pH vs $\log([\text{In}^-]/[\text{HIn}])$, we have estimated the pK_{HIn} of MOIL (Fig. S12) to be 11.53 ± 0.2 ($\text{p}K_a$ of MO is 10.6) in acetonitrile at 25 °C.²⁹

$$C_{\text{In}^-} = C_0 - C_{\text{HIn}} \quad (4)$$

Here C_0 is the initial concentration of the indicator taken; C_{In^-} and C_{HIn} are the concentration of the azo (In^-) and quinonoid (HIn) form after addition of acid respectively.

The acid equilibrium constant (pK_{HA}) of an unknown acid (HA) has been investigated by overlapping indicator methods developed by Bordwell and his groups in non-aqueous aprotic solvents (procedure is given in details in the Supporting Information).^{30, 41} Here the equilibrium acidities of some selective acids relative to that of MOIL indicator (pK_{HIn} value is known) has been measured in acetonitrile solvent by monitoring the change in the absorption spectrum of the indicator during titration process at room temperature (25°C). The acidity constants of those selective acids have been estimated according to the following equations.



$$pK_{HA} = pK_{HIn} - \log K_{eq} = pK_{HIn} - \log \frac{[A^-][HIn]}{[HA][In^-]} \quad (6)$$

During the measurements, to achieve most reliable results, we have chosen the acids in such a way that their expected pK_a values should be close enough ($< 2 pK_a$ unit) to that of the indicator. Oxygen and moisture exposure were reduced and the dilution effect was taken care of during measurements. The ion association was ignored here as the participants are in low concentrations. We have performed the calculation for at least five aliquots of each acid and found that the pK_a values calculated are almost similar during each experiment (Fig. S13). We have taken the average value of them as the result, presented in Table S1. The acid equilibrium constants determined by the MOIL indicators in this report are well supported by the literature (Table 1). Thus the IL-based indicator can also be exploited in determining the equilibrium constant of several compounds and this has been showcased for the first time using a GUMBOS in this report. So, this report has showcased a new approach where we can estimate the acid

equilibrium constant of large number of acids by preparing a series of such indicator in different solvents also.

Table 1. pK_a values for several acids determined by indicator overlapping methods.

Acids	pK_a in acetonitrile at 25 °C
Picric acid	11.2 ± 0.2 (11.0) ⁴⁰
HCl	11.4 ± 0.2 (10.3) ⁴⁰
HNO ₃	10.7 ± 0.2 (8.8) ⁵⁹
TFA	13.4 ± 0.3 (12.6) ⁵⁹
Salicylic acid	15.9 ± 0.2 (16.7) ³⁷

Conclusions

The report deals with the fabrication of an IL-based pH-responsive indicator and explores its beneficial activities compared to the free dye molecules. Here, an acid-base indicator has been synthesized by attaching the cationic backbone of the P₆₆₆₁₄Cl ionic liquid with common indicator, methyl orange. This lipophilic ionic liquid-based (GUMBOS) indicator is highly soluble in less polar solvents and exhibits good sensitivity towards the presence of acid/base in those media. Aqueous suspended nanoparticle (nanoGUMBOS) has also been developed from the IL-based indicators by simple flash nano-precipitation method. The nanoparticles are well characterized by different spectroscopic and microscopic measurements. This nanomaterial further shows better acid-base sensitive behavior in polar solvents (water) compared to free dye. So the prepared indicator displayed unique pH-responsive behavior in both the polar and non-

polar media. Further, this modified indicator has been exploited in determining the acid equilibrium constant of various acids by overlapping indicator methods in non-aqueous non-polar solvents which have been showcased for the first time here. So, the report invokes a novel approach of synthesizing a series of IL-based indicators and estimation of absolute dissociation constants of various acid-base compounds in different solvents with the help of such indicators. Further studies on similar systems involving indicators other than azo dyes are in progress.

ASSOCIATED CONTENT

Supporting Information

Detailed studies about the characterizations and discussion have been given in the Supporting Information.

CONFLICT OF INTEREST DISCLOSURE

The authors declare no competing financial interests.

ACKNOWLEDGMENTS

MH thanks SERB, Govt. of India (Fund no. SB/S1/PC-041/2013) for financial support. PP thanks DST-INSPIRE for his fellowships. RKS thanks IIT Kharagpur for financial support. SKD thanks SERB for financial support. We thank Prof. N. Sarkar for help in measuring DLS in his laboratory.

References

- 1 K. R. Seddon, *Nat. Mater.*, 2003, **2**, 363.
- 2 T. Welton, *Chem. Rev.*, 1999, **99**, 2071.
- 3 N. V. Plechkova and K. R. Seddon, *Chem. Soc. Rev.*, 2008, **37**, 123.
- 4 P. K. S. Magut, S. Das, V. E. Fernand, J. Losso, K. McDonough, B. M. Naylor, S. Aggarwal, and I. M. Warner, *J. Am. Chem. Soc.*, 2013, **135**, 15873.
- 5 D. R. MacFarlane, N. Tachikawa, M. Forsyth, J. M. Pringle, P. C. Howlett, G. D. Elliott, J. H. Davis, M. Watanabe, P. Simon, and C. A. Angell, *Energy Environ. Sci.*, 2014, **7**, 232.
- 6 R. Cannalire, M. Tiecco, V. Cecchetti, R. Germani, and G. Manfredi, *Eur. J. Org. Chem.*, 2018, **2018**, 2977.
- 7 Z. Q. He and P. Alexandridis, *Phys.Chem.Chem.Phys.*, 2015, **17**, 18238.
- 8 W. I. S. Galpothdeniya, K. S. McCarter, S. L. De Rooy, B. P. Regmi, S. Das, F. Hasan, A. Tagge, and I. M. Warner, *RSC Adv.*, 2014, **4**, 7225.
- 9 J. Kuchlyan, N. Kundu, and N. Sarkar, *Curr. Opin. Colloid Interface Sci.*, 2016, **25**, 27.
- 10 Z. M. Xue, L. Qin, J. Y. Jiang, T. C. Mu, and G. H. Gao, *Phys.Chem.Chem.Phys.*, 2018, **20**, 8382.
- 11 W. I. S. Galpothdeniya, F. R. Fronczek, M. Y. Cong, N. Bhattarai, N. Siraj, and I. M. Warner, *J. Mater. Chem. B*, 2016, **4**, 1414.
- 12 I. M. Warner, B. El-Zahab, and N. Siraj, *Anal. Chem.*, 2014, **86**, 7184.
- 13 C. N. R. Rao and A. K. Cheetham, *J. Mater. Chem.*, 2001, **11**, 2887.
- 14 S. Kayal, A. Mandal, P. Pramanik, and M. Halder, *J. Photochem. Photobiol. A*, 2019, **373**, 182.
- 15 G. Sahay, J. O. Kim, A. V. Kabanov, and T. K. Bronich, *Biomaterials*, 2010, **31**, 923.
- 16 K. S. Egorova, E. G. Gordeev, and V. P. Ananikov, *Chem. Rev.*, 2017, **117**, 7132.
- 17 M. Galluzzi, S. Bovio, P. Milani, and A. Podesta, *J. Phys. Chem. C* 2018, **122**, 7934.
- 18 M. Antonietti, D. B. Kuang, B. Smarsly, and Z. Yong, *Angew. Chem. Int.*, 2004, **43**, 4988.
- 19 J. Z. Du, X. J. Du, C. Q. Mao, and J. Wang, *J. Am. Chem. Soc.*, 2011, **133**, 17560.
- 20 H. Kasai, T. Murakami, Y. Ikuta, Y. Koseki, K. Baba, H. Oikawa, H. Nakanishi, M. Okada, M. Shoji, M. Ueda, H. Imahori, and M. Hashida, *Angew. Chem. Int.*, 2012, **51**, 10315.
- 21 P. Gouma, G. Sberveglieri, R. Dutta, J. W. Gardner, and E. L. Hines, *Mrs Bull.*, 2004, **29**, 697.
- 22 J. W. Gardner and P. N. Bartlett, *Sensor. Actuat. B-Chem.*, 1994, **18**, 211.
- 23 B. A. Suslick, L. Feng, and K. S. Suslick, *Anal. Chem.*, 2010, **82**, 2067.
- 24 L. A. Feng, C. J. Musto, J. W. Kemling, S. H. Lim, W. X. Zhong, and K. S. Suslick, *Anal. Chem.*, 2010, **82**, 9433.
- 25 Y. Wang, H. Xiong, X. Zhang, and S. Wang, *Microchim. Acta*, 2010, **170**, 27–32.
- 26 B. Luo, Y. M. Xia, H. L. Zhao, and Y. P. Wang, *Poly. Chem.*, 2015, **6**, 8099.
- 27 K. Behera, S. Pandey, A. Kadyan, and S. Pandey, *Sensors*, 2015, **15**, 30487.
- 28 M. C. Buzzeo, C. Hardacre, and R. G. Compton, *Anal. Chem.*, 2004, **76**, 4583–4588.
- 29 I. M. Kolthoff, Chantoon.Mk, and S. Bhowmik, *Anal. Chem.*, 1967, **39**, 315.
- 30 W. S. Matthews, J. E. Bares, J. E. Bartmess, F. G. Bordwell, F. J. Cornforth, G. E. Drucker, Z. Margolin, R. J. McCallum, G. J. Mccollum, and N. R. Vanier, *J. Am. Chem. Soc.*, 1975, **97**, 7006.
- 31 E. Rossini, A. D. Bochevarov, and E. W. Knapp, *ACS Omega*, 2018, **3**, 1653.
- 32 S. N. Park, H. Kim, K. Kim, J. A. Lee, and D. S. Lho, *Phys. Chem. Chem. Phys.*, 1999, **1**, 1893.
- 33 T. Matsui, T. Baba, K. Kamiya, and Y. Shigeta, *Phys. Chem. Chem. Phys.*, 2012, **14**, 4181.
- 34 A. Kutt, I. Leito, I. Kaljurand, L. Soovali, V. M. Vlasov, L. M. Yagupolskii, and I. A. Koppel, *J. Org. Chem.*, 2006, **71**, 2829.
- 35 I. M. Kolthoff, S. Bruckenstein, and M. K. Chantooni, *J. Am. Chem. Soc.*, 1961, **83**, 3927–3935.
- 36 G. Garrido, E. Koort, C. Rafols, E. Bosch, T. Rodima, I. Leito, and M. Roses, *J. Org. Chem.*, 2006, **71**, 9062.
- 37 H. S. Kim, T. D. Chung, and H. Kim, *J. Electroanal. Chem.*, 2001, **498**, 209.

- 38 W. C. Barrette, H. W. Johnson, and D. T. Sawyer, *Anal. Chem.*, 1984, **56**, 1890.
 39 C. Reichardt, *Chem. Rev.*, 1994, **94**, 2319.
 40 A. Kutt, S. Selberg, I. Kaljurand, S. Tshepelevitsh, A. Heering, A. Darnell, K. Kaupmees, M.
 Piirsalu, and I. Leito, *Tetrahedron Lett.*, 2018, **59**, 3738.
 41 G. Jakab, C. Tancon, Z. G. Zhang, K. M. Lippert, and P. R. Schreiner, *Org. Lett.*, 2012, **14**, 1724.
 42 P. Pramanik, S. K. Das, and M. Halder, *J. Phys. Chem. C*, 2020, **124**, 4791.
 43 P. Yu, *Biopolymer*, 2010, pp. 535.
 44 J. J. Murcia, M. C. Hidalgo, J. A. Navio, J. Arana, and J. M. Dona-Rodriguez, *Appl. Catal. B-
 Environ.*, 2014, **150**, 107.
 45 S. Das, P. K. S. Magut, S. L. de Rooy, F. Hasan, and I. M. Warner, *RSC Adv.*, 2013, **3**, 21054.
 46 J. Martak, T. Liptaj, and S. Schlosser, *J. Chem. Eng. Data*, 2019, **64**, 2973.
 47 S. Schlosser, J. Martak, and M. Blahusiak, *Chem. Pap.*, 2018, **72**, 567.
 48 M. G. Freire, P. J. Carvalho, R. L. Gardas, L. N. B. F. Santos, I. M. Marrucho, and J. A. P.
 Coutinho, *J. Chem. Eng. Data*, 2008, **53**, 2378–2382.
 49 A. Yadav and S. Pandey, *J. Chem. Eng. Data*, 2014, **59**, 2221.
 50 B. C. O'Kelly, *Dry. Technol.*, 2004, **22**, 1767.
 51 M. Blahusiak and S. Schlosser, *J. Chem. Thermodyn.*, 2014, **72**, 54.
 52 J. R. Lakowicz, *Springer*, 2006, **3rd ed.**
 53 A. Peters and B. C. Redmon, *J. Chem. Educ.*, 1940, **17**, 525.
 54 G. N. Smith, *Phys. Chem. Chem. Phys.*, 2018, **20**, 18919.
 55 W. W. He, L. W. Mi, L. Z. Zhang, and Z. Zheng, *Nanoscale*, 2012, **4**, 3162.
 56 D. Majhi, S. K. Das, P. K. Sahu, S. M. Pratik, A. Kumar, and M. Sarkar, *Phys. Chem. Chem.
 Phys.*, 2014, **16**, 18349.
 57 A. Mishra, R. K. Behera, P. K. Behera, B. K. Mishra, and G. B. Behera, *Chem. Rev.*, 2000, **100**,
 1973.
 58 M. Pal, A. Yadav, and S. Pandey, *Langmuir*, 2017, **33**, 9781.
 59 J. T. Muckerman, J. H. Skone, M. Ning, and Y. Wasada-Tsutsui, *Biochim. Biophys. Acta*, 2013,
1827, 882.

Graphical abstract

